Evidence for the $S=9$ excited state in Mn_{12}-bromoacetate measured by electron paramagnetic resonance

K. Petukhov and S. Hill*
Department of Physics, University of Florida, Gainesville, Florida 32611-8440, USA

N. E. Chakov, K. A. Abboud, and G. Christou
Department of Chemistry, University of Florida, Gainesville, Florida 32611-7200, USA
(Received 18 March 2004; published 31 August 2004)

We present high-frequency high-field electron paramagnetic resonance (EPR) measurements on the $[Mn_{12}O_{12}(O_2CCH_2Br)_{16}(H_2O)_4\cdot 4CH_2Cl_2]$ dodecanuclear manganese complex (Mn_{12}-BrAc). The crystal-field parameters are found to be very similar to those of the original compound Mn_{12}-acetate ($[Mn_{12}O_{12}(O_2CCH_3)_{16}(H_2O)_4]$). A detailed analysis of the frequency and temperature dependence of anomalous peaks observed in the EPR spectra of Mn_{12}-BrAc enables us to locate the $S=9$ manifold at about 40 K above the $M_S=\pm 10$ ground state of this nominally $S=10$ system. This is very close to the $M_S=\pm 6$ state of the $S=10$ manifold, thus suggesting pathways for the thermally assisted magnetization dynamics and related properties. Finally, the EPR fine structures recently attributed to disorder associated with the acetic acid of crystallization in Mn_{12}-Ac are absent in the present measurements, thus suggesting that the Mn_{12}-BrAc complex represents a more suitable candidate for measurements of quantum effects in high symmetry $S=10$ SMMs.

DOI: 10.1103/PhysRevB.70.054426 PACS number(s): 75.50.Xx, 75.60.Jk, 75.75.+a, 76.30.−v

In 1996, it was reported that Mn_{12}-Ac exhibits resonant magnetic quantum tunneling (MQT), as evidenced by steps that occur at regular intervals in the low-temperature hysteresis loops of the complex.[1,2] Since then, considerable interest has been devoted towards the understanding of the quantum behavior of single molecule magnets (SMMs), in particular Mn_{12}-Ac (shorthand for Mn_{12}-acetate $[Mn_{12}O_{12}(O_2CCH_3)_{16}(H_2O)_4]\cdot 2CH_3CO_2H\cdot 4H_2O$). One of the most intriguing open questions concerns whether or not one can ignore couplings to $S\neq 10$ states in any theoretical treatment of the low-temperature quantum properties of Mn_{12}-Ac (including MQT). For example, recently a low lying$S=9$ excited state was found in Fe_8Br_8, another SMM with a $S=10$ ground state.[3] In this paper we provide clear experimental evidence for a $S=9$ excited state of the nominally $S=10$ single-molecule magnet Mn_{12}-BrAc (shorthand for Mn_{12}-bromoacetate $[Mn_{12}O_{12}(O_2CCH_2Br)_{16}(H_2O)_4]\cdot 4CH_2Cl_2$), a closely related complex to Mn_{12}-Ac.

Like Mn_{12}-Ac, which remains the most widely studied SMM,[4,5] Mn_{12}-BrAc crystallizes in a tetragonal space group with individual molecules possessing S_4 site symmetry. Selection rules for quantum tunneling of the magnetization imposed by the S_4 crystallographic symmetry are not strictly obeyed by Mn_{12}-BrAc or Mn_{12}-Ac, however.[6] A number of explanations have been proposed to account for this anomalous behavior, including crystal dislocations[7] and, more recently, disordered solvent molecules of crystallization that give rise to symmetry breaking effects.[6,8–10] Cornia *et al.* have proposed that the fourfold (S_4) molecular symmetry is disrupted by a strong hydrogen-bonding interaction between an acetate ligand of the Mn_{12} cluster and a disordered acetic acid molecule of crystallization.[10] Using their model, up to six isomers can exist in the lattice, each of which differs in the number and arrangement of hydrogen-bonding interactions. Of the six isomers, only two have crystallographic fourfold (S_4) symmetry. The remaining four isomers have lower symmetry and can explain many experimental factors associated with the low temperature hysteresis loops of the complex, including odd-to-even M_S MQT steps. It is therefore of importance to study the magnetic behavior of a high symmetry Mn_{12} cluster that consist of only one species with strict axial symmetry. The only other known complex to date that meets these specifications is Mn_{12}-BrAc. The core of the molecule is the same as that of Mn_{12}-Ac and the molecule also possesses a spin $S=10$ ground state. The complex is therefore an ideal candidate for study, as there are four relatively inert CH_2Cl_2 (dichloromethane) solvent molecules per Mn_{12}-BrAc molecule. This is in contrast to the strongly hydrogen-bonding nature of the water and acetic acid molecules of crystallization in the case of Mn_{12}-Ac. However, like all other known Mn_{12}-based SMMs, all tunneling resonances are observed, including odd-to-even M_S MQT steps.[11] Recently, del Barco *et al.* proposed that a distribution of internal transverse magnetic fields in Mn_{12}-BrAc is responsible for a lack of any selection rules in the MQT phenomena.[11]

The Mn_{12}-BrAc molecule consists of four Mn^{4+} ions, each with spin $S=\frac{3}{2}$, surrounded by eight Mn^{3+} ions with spin $S=2$.[4,5] The orbital moment is quenched, and a Jahn-Teller distortion associated with the Mn^{3+} ions is largely responsible for the magnetic anisotropy. A simplified treatment of the magnetic interactions within the molecule has been developed[12–16] wherein four strongly antiferromagnetically coupled Mn^{3+}-Mn^{4+} dimers, each with spin $S=2-\frac{3}{2}=\frac{1}{2}$, couple via an effective ferromagnetic interaction to the four remaining $S=2$ Mn^{3+} ions, giving a total spin $S=10$. The magnetic energy levels of the rigid $S=10$ spin system are then usually described by the effective single-spin Hamiltonian,[17,18]

$$\hat{H} = D\hat{S}_z^2 + \mu_B \vec{B} \cdot \vec{\vec{g}} \cdot \hat{S} + \hat{H}', \quad (1)$$

where $D(<0)$ is the uniaxial anisotropy constant, the second term represents the Zeeman interaction with an applied field $\vec{B}$ ($\vec{\vec{g}}$ is the Landé g tensor), and $\hat{H}'$ includes higher order terms in the crystal field ($\hat{O}_4^0$, $\hat{O}_2^2$, $\hat{O}_4^2$, $\hat{O}_4^4$, etc.), as well as environmental couplings such as intermolecular dipolar and exchange interactions.[19,20] The leading term in Eq. (1) is responsible for the energy barrier to magnetization reversal and the resulting magnetic bistability.[4,5] The weaker couplings between the four spin-$\frac{1}{2}$ dimers and the four spin-2 Mn^{3+} ions largely determine the low energy excitations within the molecule (to $S \neq 10$ states).[12,14] However, the nature of these couplings is not well known.

The inadequacy of the $S=10$ model was perhaps first raised by Caneschi *et al.* in order to interpret the temperature dependent susceptibility of Mn_{12}-Ac.[21] Their calculation proposed the existence of two degenerate $S=9$ states at 0.725 THz (~35 K), one $S=8$ state at 1.195 THz (~57 K), and other $S \leqslant 8$ and $S > 10$ states at higher energies. Not all of these states, however, were clearly observed in the inelastic neutron scattering study of Mn_{12}-Ac, where a well-pronounced mode was found at around 1.2 THz, while the mode at 0.725 THz was hardly visible and the authors attributed this fact to a very small intensity at the corresponding scattering vector.[22] Magnetization measurements have shown the existence of $S \leqslant 9$ excited levels at energies between 30 and 90 K.[23] Furthermore, measurements of the Mn_{12}-Ac transmission spectra in the submillimeter range indicate the existence of some weak band around $30-35\ cm^{-1}$ (~43–50 K) at high temperatures, whose frequencies do not match the transitions within the ground $S=10$ multiplet.[24] Finally, by means of ^2D and ^{13}C NMR investigations[25,26] and ^{55}Mn spin-lattice relaxation measurements[12] it has also been clearly established that the unpaired electron density is distributed over the entire Mn_{12}-Ac framework. These challenging experimental findings stimulated subsequent calculations, which placed the $S=9$ manifold at 35 K or higher.[14,16,27] All of these observations provided the impetus for the present undertaking—a detailed investigation of the spin-energy levels of a Mn_{12} cluster by variable frequency, variable temperature EPR spectroscopy. We provide definitive evidence for the existence of a state at 40 ± 2 K with all of the properties of an $S=9$ manifold. The results help the understanding of many of the above-mentioned features and are in good agreement with more recent high precision electronic structure calculations.[27]

Multi-high-frequency (51.5, 65.4, and 76.9 GHz) single crystal EPR measurements were carried out using a millimeter-wave vector network analyzer (MVNA) and a high sensitivity cavity perturbation technique; this instrumentation is described in detail elsewhere.[28] The measurements were performed using a commercial superconducting solenoid capable of producing fields of up to 9 T. In all cases, the temperature was stabilized (±0.01 K) relative to a calibrated Cernox™ resistance sensor. We have outfitted our cavities with rotatable endplates for sample orientation with 0.18° resolution.[29] The single-crystal sample was optimally positioned and oriented for high-field EPR measurements on the fundamental TE01*n* modes (n=integer) of the cavity, and for DC field (**B**) alignment close to the hard plane of the sample, i.e., with the AC excitation field (H_1) along the z axis of the crystal ($\perp$ to **B**). Submillimeter-sized single Mn_{12}-BrAc crystals were prepared from $Mn_{12}O_{12}(O_2CMe)_{16}(H_2O)_4$ (Mn_{12}-acetate) by a ligand substitution procedure involving the treatment of Mn_{12}-Ac with an excess of $BrCH_2CO_2H$ in two cycles. Repeated treatment is necessary as the ligand substitution reaction is an equilibrium process that must be driven to completion if the pure product is to be obtained.[30–32] The initial complex Mn_{12}-Ac was synthesized using standard methods.[33] In order to confirm the solvent content of $4CH_2Cl_2$ per formula unit, an x-ray structural refinement analysis was carried out on a wet single-crystal removed directly from the mother liquor. In order to avoid solvent loss in the EPR measurements, the sample was removed from the mother liquor, immediately sealed in silicone grease, and quickly transferred to the cryostat (ca. 5 minutes) where it was cooled under atmospheric pressure helium gas. Similar sample handling procedures have been carried out for Mn_{12} samples containing considerably more volatile solvent molecules, and these have shown minimal solvent loss, as verified by before and after AC SQUID measurements.[34]

In order to align the sample's hard plane (x,y) with respect the applied DC magnetic field, angle dependent measurements of the EPR spectra were performed, as shown in Fig. 1(a). In general, the hard-plane spectra of Mn_{12}-BrAc look very similar to those of Mn_{12}-Ac.[35,36] In the high-field limit ($g\mu_B \mathbf{B} > |D|S$), one expects a total of 20 EPR transitions within the $2S+1(S=10)$ multiplet, as shown in Fig. 1(b) by solid curves. The α resonances, which correspond to transitions within the Zeeman-split $M_S = \pm m$ (m=integer, and $0 \leqslant m \leqslant S$) zero-field levels, comprise half of this total; in the zero-field limit, the quantization axis is defined by the uniaxial crystal field tensor, and is along z. In the high-field limit, the quantization axis points along the applied field vector; the 10 α resonances then correspond to transitions from M_S=even-to-odd m, e.g., $M_S=-10$ to -9. Because the α resonances originate from pairs of levels ($\pm m$) which are (approximately) degenerate in zero field, one expects the resonance frequencies, when plotted against field, to tend to zero as the field tends to zero, as can be seen in Fig. 1(c). The simulation depicted in Fig. 1(c) has been performed by exact diagonalization of Eq. (1), and this procedure is described in detail elsewhere.[35,36] In order to fit our experimental data (open circles), we have used crystal field (CF) parameters obtained from our earlier studies of Mn_{12}-BrAc with the field along the easy axis:[37] $D=-0.456\ cm^{-1}$, $B_4^0 = -2.0 \times 10^{-5}\ cm^{-1}$. These Hamiltonian parameters are very close to the accepted CF parameters for Mn_{12}-Ac ($D = -0.454\ cm^{-1}$, $B_4^0 = -2.0 \times 10^{-5}\ cm^{-1}$),[8,18,36] thus emphasizing the close similarity of physical properties of these two derivatives of the $Mn_{12}O_{12}$ molecule.

In earlier investigations of Mn_{12}-Ac it was pointed out that EPR spectra obtained for a field applied perpendicular to the easy axis of the molecule revealed a number of anomalous transitions which were labeled β,[35,36] as opposed to the

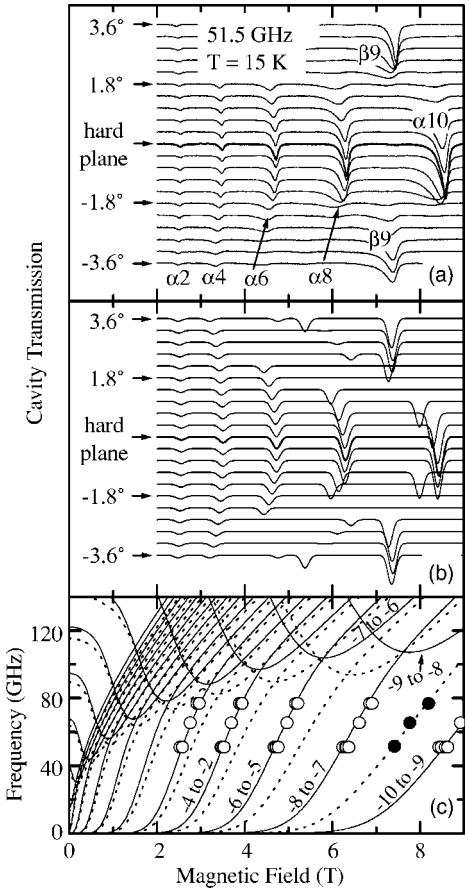

FIG. 1. (a) Angle dependence of the EPR spectra of Mn_{12}-BrAc in the range of ±3.6° either side of the hard plane, with an angular step of 0.36°. (b) The SIM (Ref. 39) simulations of the EPR spectra for the field tilted up to ±3.6° away from the hard plane. (c) Fits to Eq. (1) for the frequency dependence of the hard plane spectra for the $S=10$ state (solid curves, open circles) and for the $S=9$ state (dotted curves, solid circles); the CF parameters for this simulation are given in the text. Open and closed circles are experimental data at frequencies of 51.5, 65.4, and 76.9 GHz.

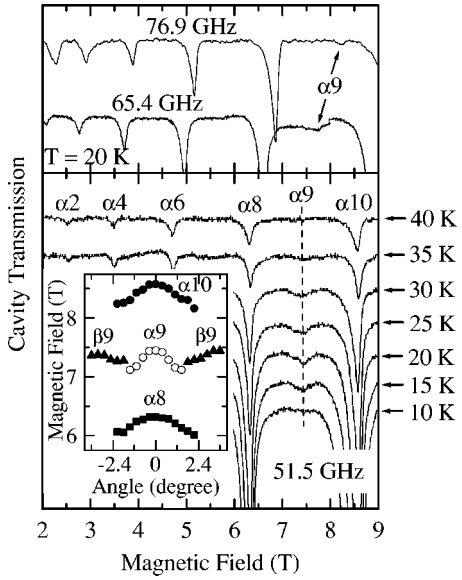

FIG. 2. (Top panel) Typical single-crystal EPR spectra for Mn_{12}-BrAc at 65.4 and 76.9 GHz ($\mathbf{B}\perp z$), the $\alpha 9$ resonance is evidenced at high fields for both frequencies. (Bottom panel) Temperature dependence of the EPR spectra of Mn_{12}-BrAc at 51.5 GHz ($\mathbf{B}\perp z$). Inset, angle dependence of several of the most important resonances.

α resonances which nicely fit the accepted $S=10$ Hamiltonian [Eq. (1)].[38] Initially, these β transitions were tentatively ascribed to the M_S=odd-to-even transitions (e.g., $M_S=-9$ to -8);[35] however we note here that they should not be observable below a cutoff frequency, which is about 95 GHz at high fields for the given CF parameters, as depicted in Fig. 1(c). In full agreement with these calculations we do not observe these β resonances until we slightly misalign the sample's hard plane with respect to the applied magnetic field [Fig. 1(a)]. Indeed, at ±3.6° away from the hard plane, the β resonances become highly pronounced. Meanwhile, the $\alpha 10$, $\alpha 8$, and $\alpha 6$ resonances disappear over this same angle range, as shown in Fig. 1(a). In fact, there is an approximately 0.75° range over which neither $\alpha 10$ or $\beta 9$ are observed and, although $\alpha 4$ and $\alpha 2$ peaks remain visible at $\theta=\pm 3.6°$, it is clear that their intensities diminish substantially. This symmetry effect between the out-of-plane angle dependence of the β and α resonances was recently reported for Mn_{12}-Ac, and is discussed in more detail in Ref. 9. For comparison, Fig. 1(b) shows simulations of the EPR spectra for the same angle range, generated using the program SIM.[39] These simulations agree well with our observations, i.e., the α peaks disappear, and $\beta 9$ appears, as the field is tilted away from the hard plane. Indeed, the simulations predict quite accurately the angles at which the α peaks switch off, and $\beta 9$ switches on. This contrasts the behavior seen in Mn_{12}-Ac, where a significant overlap of the α and β peaks has been attributed to a distribution of tilts of the easy axes of the molecules (up to ±1.7°), induced by a discrete disorder associated with the two acetic acids of crystallization.[9] A small distribution of tilts can be inferred from the present data, as seen from the overlap of the $\alpha 10$ and $\beta 9$ resonances (inset Fig. 2), and from the absence of some of the features in the simulations which disperse strongly with angle. However, the width of the distribution must be on the order of, or less than, the angle resolution employed in these measurements, i.e., $\sim\pm 0.2°$. This suggests that the distributions of transverse fields recently reported by del Barco *et al.* must have an explanation unrelated to easy axis tilting. It is also apparent from the data in Fig. 1(a) that, for the most part, the resonances are extremely symmetric and much sharper than those observed for Mn_{12}-Ac (see Ref. 9). In particular, none of the fine structures seen in the hard axis spectra of Mn_{12}-Ac are seen for the present complex; e.g., the pronounced high-field shoulders on the α resonances. Consequently, we can conclude that the discrete solvent disorder[6,8–10] that is now well established in Mn_{12}-Ac is absent in Mn_{12}-BrAc. This observation is consistent with the full compliment of four solvent molecules per formula unit, and suggests that the BrAc complex probably represents a more suitable candidate for measurements of quantum effects in high symmetry $S=10$ SMMs.

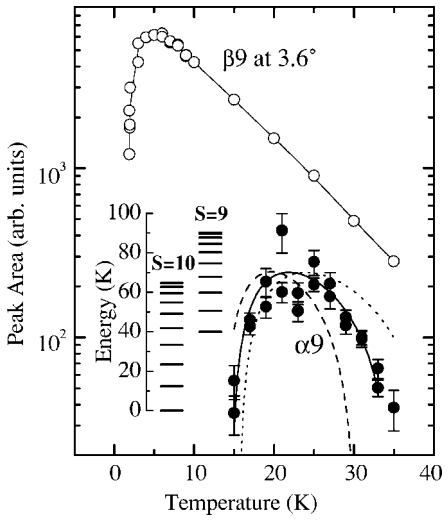

FIG. 3. Temperature dependence of the area of the $\alpha 9$ (solid circles) and $\beta 9$ (open circles) resonances. The solid line through the open circles is a guide to the eye. The curves through the solid circles represent the calculated $\alpha 9$-resonance areas assuming $\Delta = 36$ K (dashed), $\Delta = 40$ K (solid), and $\Delta = 44$ K (dotted). Inset, schematic for the energy levels of both the $S=10$ and $S=9$ states in zero magnetic field. $S=9$ is located at an energy $\Delta = 40 \pm 2$ K above the bottom of the $S=10$ state.

In Fig. 2 (bottom panel) we present the temperature dependence of the EPR spectra of Mn_{12}-BrAc at 51.5 GHz for a field applied perpendicular to the easy axis of the crystal ($\mathbf{B} \perp z$) to within an accuracy of $\pm 0.1°$, as inferred from the angle dependent data in Fig. 1. As the temperature is increased from 10 K up to 40 K, an extra resonance is found at 7.42 T. Since this peak is located between the $\alpha 10$ and $\alpha 8$ resonances, we have labeled this resonance $\alpha 9$. We have also observed similar peaks at 65.4 and 76.9 GHz, which are located, respectively, at 7.77 and 8.22 T, i.e., between the $\alpha 8$ and $\alpha 10$ peaks. We have plotted the positions of $\alpha 9$ versus frequency in Fig. 1(c) (solid circles). It is tempting to attribute these α resonances to the onset of the $\beta 9$ transitions, which could occur if a small minority of molecules have their easy axes tilted with respect to the majority of molecules, whose easy axes are exactly perpendicular to applied magnetic field, as has recently been found for Mn_{12}-Ac.[9] However, a careful angle-dependent study of the EPR spectra shows that the positions of $\alpha 9$ and $\beta 9$ exhibit completely different angle dependencies, as shown in the inset of Fig. 2. The temperature dependencies of the intensities of the $\alpha 9$ and $\beta 9$ peaks reveal even more discrepancies. We have calculated the areas under the $\alpha 9$ and $\beta 9$ peaks and plotted them as a function of temperature, as represented in Fig. 3 by solid and open circles, respectively. The area under the peaks was calculated by integration using the trapezoidal rule. This procedure does not employ any fitting functions and is sensitive only to the noise background of the data, the corresponding uncertainty is depicted by error bars in Fig. 3. Again, the nature of the $\alpha 9$ resonance is different from the $\beta 9$ resonance and, thus, the $\alpha 9$ resonance cannot be explained within the framework of the $S=10$ picture.

Further examination of Figs. 2 and 3 reveals that the $\alpha 9$ resonance diminishes in intensity as the temperature decreases to 15 K, becoming invisible at 10 K. This fact proves beyond any doubt that the $\alpha 9$ resonance originates from an excited state of the Mn_{12}-BrAc molecule. We therefore conclude that, at low frequencies, the $\alpha 9$ resonance corresponds to a transition within an excited state of Mn_{12}-BrAc. For comparison, Fig. 1(c) includes dashed curves corresponding to fits to the $\alpha 9$ data; this fit assumes $S=9$ and, due to the limited number of data points, allows only for the variation of D. For an odd total spin state, the low field limiting behavior of odd-to-even m and even-to-odd m transitions is the reverse of that for an even total spin state. Consequently, one does expect the frequency of the $M_S = -9$ to -8 transition to go to zero in the low field limit within the $S=9$ manifold. The fit to the data for $S=9$ yields the Hamiltonian parameter $D = -0.430$ cm^{-1}(-0.62 K), which is thus 5% smaller than for $S=10$. The low frequency $\alpha 9$-resonance data lie perfectly on the $S=9$ curves. Therefore, the anisotropy barrier for the $S=9$ state is $|D|S^2 \approx 50$ K, which is 23% smaller than that for $S=10$(65 K). Having established that the low-frequency $\alpha 9$ transition corresponds to an $S=9$ state, we can estimate its approximate location relative to $S=10$. Using the CF parameters for both $S=10$ and $S=9$ states we were able to calculate the energy levels $E_{10}(m_S)$ and $E_9(m_S)$ for the two states, and both partition functions $Z_{10}(m_s) = \Sigma_{m_S=-10}^{10} e^{-E_{10}(m_S)/T}$ and $Z_9(m_s) = \Sigma_{m_S=-9}^{9} e^{(-E_9(m_S)+\Delta)/T}$, for a given temperature T, where Δ is the energy difference between the bottoms of the $S=10$ and $S=9$ manifolds. The area under the $\alpha 9$ peak, at a given temperature, is proportional to the difference of populations of the corresponding levels:

$$A_{\alpha 9}(\Delta, T) \propto \frac{N_{-9} - N_{-8}}{Z} = \frac{e^{\{E_9(-8) - E_9(-9)\}/T}}{Z_{10}(T) + Z_9(\Delta, T)}.$$

Thus, by varying the only parameter Δ, we have found that the $S=9$ manifold is located at $\Delta = 40 \pm 2$ K above the bottom of the $S=10$ state (see inset of Fig. 3). This implies that the $S=9$ state lies very close to the $M_S = \pm 6$ excited state within the $S=10$ multiplet. We have also performed similar calculations of the temperature dependence of the $\alpha 9$-peak area for the values of $\Delta = 36$ K and $\Delta = 44$ K, and both dependencies were inconsistent with our experimental data, as depicted in Fig. 3. The obtained location of the $S=9$ excited state at $\Delta = 40 \pm 2$ K is in perfect agreement with recent calculations.[27]

In summary, detailed frequency and temperature dependent EPR studies of Mn_{12}-BrAc reveal the existence of an $S=9$ state located only 40 ± 2 K above the $S=10$, $M_S = \pm 10$ ground state. This result is in perfect agreement with theoretical predictions.[14,27] The effects of the coexistence of an excited $S=9$ state and the ground $S=10$ state in the Mn_{12} molecule are not known, and we hope these investigations will stimulate further theoretical studies. Our experiments also indicate that Mn_{12}-BrAc is an intrinsically cleaner system than Mn_{12}-Ac, which we believe to be connected with the fact that the former possesses a full compliment of four solvent molecules per formula unit. Thus, future investiga-

tions of the title compound may provide further insights into the quantum magnetization dynamics of giant spin ($S=10$) SMMs.

The authors thank N. S. Dalal, E. Rumberger, D. N. Hendrickson, E. del Barco, A. D. Kent, and W. Wernsdorfer for useful discussion. This work was supported by the NSF (DMR0103290, DMR0239481, and CHE0123603). S. H. acknowledges the Research Corporation for financial support.

*Corresponding author. Email address: hill@phys.ufl.edu

[1] J. R. Friedman, M. P. Sarachik, J. Tejada, and R. Ziolo, Phys. Rev. Lett. **76**, 3830 (1996).
[2] L. Thomas, F. Lionti, R. Ballou, D. Gatteschi, R. Sessoli, and B. Barbara, Nature (London) **383**, 145 (1996).
[3] D. Zipse, J. M. North, N. S. Dalal, S. Hill, and R. S. Edwards, Phys. Rev. B **68**, 184408 (2003).
[4] G. Christou, D. Gatteschi, D. N. Hendrickson, and R. Sessoli, MRS Bull. **25**, 66 (2000).
[5] D. Gatteschi and R. Sessoli, Angew. Chem. **42**, 268 (2003).
[6] E. del Barco, A. D. Kent, E. M. Rumberger, D. N. Hendrickson, and G. Christou, Phys. Rev. Lett. **91**, 047203 (2003).
[7] D. A. Garanin and E. M. Chudnovsky, Phys. Rev. B **65**, 094423 (2002).
[8] S. Hill, R. S. Edwards, S. I. Jones, N. S. Dalal, and J. M. North, Phys. Rev. Lett. **90**, 217204 (2003).
[9] S. Takahashi, R. S. Edwards, J. M. North, S. Hill, and N. S. Dalal, Phys. Rev. B (to be published).
[10] A. Cornia, R. Sessoli, L. Sorace, D. Gatteschi, A. L. Barra, and C. Daiguebonne, Phys. Rev. Lett. **89**, 257201 (2002); A. Cornia, A. C. Fabretti, R. Sessoli, L. Sorace, D. Gatteschi, A.-L. Barra, C. Daiguebonned, and T. Roisnele, Acta Crystallogr., Sect. A: Found. Crystallogr. **58**, m371 (2002).
[11] E. del Barco, A. D. Kent, N. E. Chakov, L. N. Zakharov, A. L. Rheingold, D. N. Hendrickson, and G. Christou, Phys. Rev. B **69**, 020411 (2004).
[12] S. Yamamoto and T. Nakanishi, Phys. Rev. Lett. **89**, 157603 (2002).
[13] R. Sessoli, H.-L. Tsai, A. R. Schake, S. Wang, J. B. Vincent, K. Folting, D. Gatteschi, G. Christou, and D. N. Hendrickson, J. Am. Chem. Soc. **115**, 1804 (1993).
[14] M. I. Katsnelson, V. V. Dobrovitski, and B. N. Harmon, Phys. Rev. B **59**, 6919 (1999).
[15] C. Raghu, I. Rudra, D. Sen, and S. Ramasesha, Phys. Rev. B **64**, 064419 (2001).
[16] N. Regnault, Th. Jolicoeur, R. Sessoli, D. Gatteschi, and M. Verdaguer, Phys. Rev. B **66**, 054409 (2002).
[17] A. L. Barra, D. Gatteschi, and R. Sessoli, Phys. Rev. B **56**, 8192 (1997).
[18] I. Mirebeau, M. Hennion, H. Casalta, H. Andres, H. U. Güdel, A. V. Irodova, and A. Caneschi, Phys. Rev. Lett. **83**, 628 (1999).
[19] S. Hill, S. Maccagnano, K. Park, R. M. Achey, J. M. North, and N. S. Dalal, Phys. Rev. B **65**, 224410 (2002).
[20] K. Park, M. A. Novotny, N. S. Dalal, S. Hill, and P. A. Rikvold, Phys. Rev. B **66**, 144409 (2002).
[21] A. Caneschi, D. Gatteschi, L. Pardi, and R. Sessoli, in *Perspectives in Coordination Chemistry*, edited by A. F. Williams, C. Floriani, and A. E. Merbach (VCH, Basel, 1992), p. 109.
[22] M. Hennion, L. Pardi, I. Mirebeau, E. Suard, R. Sessoli, and A. Caneschi, Phys. Rev. B **56**, 8819 (1997).
[23] B. Barbara, L. Thomas, F. Lionti, A. Sulpice, and A. Caneschi, J. Magn. Magn. Mater. **177–181**, 1324 (1998).
[24] A. A. Mukhin, V. D. Travkin, A. K. Zvezdin, S. P. Lebedev, A. Caneschi, and D. Gatteschi, Europhys. Lett. **44**, 778 (1998).
[25] R. M. Achey, P. L. Kuhns, A. P. Reyes, W. G. Moulton, and N. S. Dalal, Phys. Rev. B **64**, 064420 (2001).
[26] R. M. Achey, P. L. Kuhns, A. P. Reyes, W. G. Moulton, and N. S. Dalal, Solid State Commun. **121**, 107 (2002).
[27] K. Park, M. R. Pederson, and C. S. Hellberg, Phys. Rev. B **69**, 014416 (2004).
[28] M. Mola, S. Hill, P. Goy, and M. Gross, Rev. Sci. Instrum. **71**, 186 (2000).
[29] S. Takahashi and S. Hill, Rev. Sci. Instrum. (unpublished).
[30] M. Soler, P. Artus, K. Folting, J. C. Huffman, D. N. Hendrickson, and G. Christou, Inorg. Chem. **40**, 4902 (2001).
[31] J. An, Z.-D. Chen, X.-X. Zhang, H. G. Raubenheimer, C. Esterhuysen, S. Gao, and G.-X. Xu, J. Chem. Soc. Dalton Trans. **22**, 3352 (2001).
[32] H.-L. Tsai, D.-M. Chen, C.-I. Yang, T.-Y. Jwo, C.-S. Wur, G.-H. Lee, and Y. Wang, Inorg. Chem. Commun. **4**, 511 (2001).
[33] T. Lis, Acta Crystallogr., Sect. B: Struct. Crystallogr. Cryst. Chem. **36**, 2042 (1980).
[34] M. Soler, R. S. Edwards, and S. Hill (unpublished).
[35] S. Hill, J. A. A. J. Perenboom, N. S. Dalal, T. Hathaway, T. Stalcup, and J. S. Brooks, Phys. Rev. Lett. **80**, 2453 (1998).
[36] S. Hill, R. S. Edwards, J. M. North, S. Maccagnano, and N. S. Dalal, Polyhedron **22**, 1897 (2003); also R. S. Edwards, S. Hill, S. Maccagnano, J. M. North, and N. S. Dalal, arXiv: cond-mat/0302052.
[37] R. S. Edwards, S. Hill, N. E. Chakov, and S. Hill (unpublished).
[38] We note that this numbering convention differs slightly from the scheme used in earlier publications. We previously used all integers when numbering the α and β resonances (Ref. 35). This scheme ignores the obvious symmetries associated with the various transitions. Therefore, we now use only even integers for α resonances, and odd integers for β resonances, i.e., $\alpha 9$ under the old notation is now $\alpha 8$, $\beta 10$ is $\beta 9$, $\alpha 8$ is $\alpha 6$, and so on.
[39] Written by H. Weihe, University of Copenhagen, http://sophus.kiku.dk/software/epr/epr.html;see also J. Glerup and H. Weihe, Acta Chem. Scand. **45**, 444 (1991);C. J. H. Jacobsen, E. Pedersen, J. Villadsen, and H. Weihe, Inorg. Chem. **32**, 1216 (1993).